Chin. J. Chem. Eng., **15**(3) 333—338 (2007)

Dynamic Simulation of Shear-induced Particle Migration in a Two-dimensional Circular Couette Device*

YU Zhaosheng(余钊圣)[a,b,**], **SHAO Xueming**(邵雪明)[a] **and Roger Tanner**[b]
[a] Department of Mechanics, State Key Laboratory of Fluid Power Transmission and Control, Zhejiang University, Hangzhou 310027, China
[b] School of Aerospace, Mechanical and Mechatronic Engineering, University of Sydney, NSW, 2006, Australia

Abstract The shear-induced migration of neutrally-buoyant non-colloidal circular particles in a two-dimensional circular Couette flow is investigated numerically with a distributed Lagrange multiplier based fictitious domain method. The effects of inertia and volume fraction on the particle migration are examined. The results indicate that inertia has a negative effect on the particle migration. In consistence with the experimental observations, the rapid migration of particles near the inner cylinder at the early stage is observed in the simulation, which is believed to be related to the chain-like clustering of particles. The migration of circular particles in a plane Poiseuille flow is also examined in order to further confirm the effect of such clustering on the particle migration at early stage. There is tendency for the particles in the vicinity of outer cylinder in the Couette device to pack into concentric rings at late stage in case of high particle concentration.
Keywords shear-induced particle migration, dynamic simulation, circular Couette flow, clustering

1 INTRODUCTION

Numerous experiments revealed that initially uniformly distributed particles in suspension will migrate from regions of higher shear rate to regions of lower shear rate in inhomogeneous shear flows, resulting in nonuniform concentration distributions at a steady state (*e.g.*, Leighton and Acrivos[1], Abbott *et al*.[2], Lyon and Leal[3]). This phenomenon was called 'shear-induced migration'. The Couette flow between two concentric cylinders with the inner one rotating and the outer one fixed is a typical flow for studying the shear-induced particle migration. The experiments (Abbott *et al*.[2], Phillips *et al*.[4], Tetlow *et al*.[5]) showed that particles migrate outwards and the amount of migration depends basically on the number of turns and the particle diameters. The effects of the shear rate, the viscosity of solvent, the degree of polydispersity and the surface roughness are relatively insignificant.

Some constitutive equations for concentrated suspensions that accounts for shear-induced particle migration have been developed (*e.g.*, Phillips *et al*.[4], Nott and Brady[6], Fang *et al*.[7]). However, the microstructure of suspensions is overlooked in the constitutive models. The experiment of Leighton and Rampall[8] showed that there existed a predominance of chain structures aligned with the compression axis in simple shear flow, which was recognized as a mechanism for the observation that the measured transient viscosity of the suspension in the circular Couette device decreased upon the reversal of the rotational direction of the inner wall. Fig.1 plots the microstructure of a bimodal suspension in a circular Couette device in the experiment of Graham *et al*.[9], and it clearly shows that particles migrate away from the region of higher shear rate and pack into rings (or shells) at the region of relatively lower shear rate.

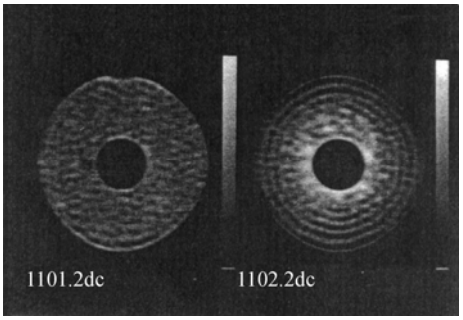

Figure 1 NMR images of a cross section of the suspension of 60% volume fraction bidisperse spheres in a circular Couette device (Left image: the initial uniform suspension; right image: the final steady state)

There are three approaches in different scales to handle the particulate flows: the macroscopic approach such as two-fluid model[10] and diffusion flux model[11], whose feature is to take the solid phase as a continuum media, the mesoscopic approach such as discrete particle model (or point particle model)[12—14], whose feature is to deal with the motion of particles individually, but to calculate the hydrodynamic forces on the particles with empirical formulas, and the microscopic approach such as the direct numerical simulation (DNS), whose feature is to determine the hydrodynamic forces on the particles from the solution of the Navier-Stokes equations or the lattice-Boltzmann equation for fluid flows outside the particles. The advantage of the direct numerical simulation (DNS) is that the hydrodynamic interactions between the fluid and the particles can be accurately determined in principle, and its disadvantage is that the computational cost is significantly larger than the macroscopic two-fluid model and the mesoscopic

Received 2006-04-14, accepted 2007-01-29.
* Supported by the National Natural Science Foundation of China (No.10472104).
** To whom correspondence should be addressed. E-mail: yuzhaosheng@zju.edu.cn

discrete particle model. With the rapid development of computer power, the direct numerical simulation (DNS) has become a practical and important tool to probe the mechanics in particulate flows. Over the past decade a variety of DNS methods have been proposed, such as the arbitrary Lagrangian-Eulerian (ALE) finite-element method (FEM)[15], the lattice-Boltzmann method (LBM)[16] and the distributed Lagrange multiplier based fictitious domain method (DLM/FD)[17]. The DLM/FD method was developed by Glowinski *et al*.[17]. The key idea in this method is that the interior domains of the particles are filled with the same fluids as the surroundings and the Lagrange multiplier (physically a pseudo body force) is introduced to enforce the interior (fictitious) fluids to satisfy the constraint of rigid body motion. The method has been successfully applied to the simulation of particulate flows[17—23].

The aim of this study is to numerically investigate the shear-induced particle migration in a two-dimensional circular Couette device by a direct simulation with the DLM/FD method.

2 NUMERICAL MODEL

2.1 Couette flow

The schematic diagram of the circular Couette flow is depicted in Fig.2. The inner cylinder rotates with Ω and the outer cylinder is fixed. The radii of the inner and outer cylinders are kR and R respectively. The particles are suspended in the fluid between the two cylinders. The experiments showed that the particles migrated away from the inner cylinder region (*i.e*., higher shear-rate region). The DLM/FD method is employed to numerically reproduce and examine this shear-induced migration phenomenon.

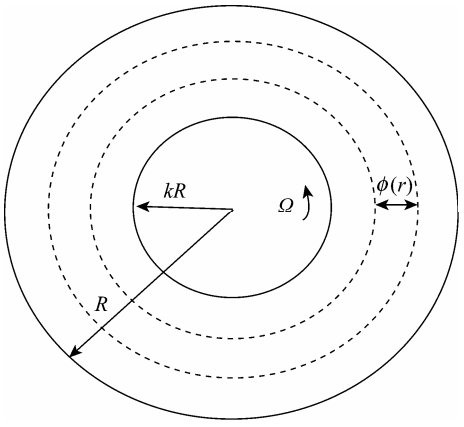

Figure 2 The schematic diagram of the circular Couette flow

2.2 DLM/FD method

The DLM/FD method was developed by Glowinski *et al*.[17], and Yu *et al*.[19—23] have made a variety of modifications on the original numerical implementation to improve the efficiency and accuracy of the method. The reader is referred to Yu *et al*.[22,23] for the detailed description of the numerical implementation that is adopted here. In the following, a brief description is given.

Let $P(t)$ represents the interior of the particle (one particle is considered for convenience of description, however, it is straightforward to extend to many-particle case). V_0 denotes the entire domain comprising the interior $P(t)$ and the exterior of the particle. The dimensionless governing equations in weak form for the incompressible fluid consist of the following two parts:

Combined momentum equations:

$$\int_{V_0}\left(\frac{\partial \boldsymbol{u}}{\partial t}+\boldsymbol{u}\cdot\nabla\boldsymbol{u}\right)\cdot\boldsymbol{v}\mathrm{d}\boldsymbol{x}= \int_{V_0}\nabla\cdot\left(-p\boldsymbol{I}+\frac{2\boldsymbol{D}}{Re}\right)\cdot\boldsymbol{v}\mathrm{d}\boldsymbol{x}+\int_{P(t)}\boldsymbol{\lambda}\cdot\boldsymbol{v}\mathrm{d}\boldsymbol{x} \tag{1}$$

$$(\rho_{\mathrm{r}}-1)\left[V_{\mathrm{P}}^{*}\left(\frac{\mathrm{d}\boldsymbol{U}}{\mathrm{d}t}-Fr\right)\cdot\boldsymbol{V}+J^{*}\frac{\mathrm{d}\boldsymbol{\omega}}{\mathrm{d}t}\cdot\boldsymbol{\xi}\right]= -\int_{P(t)}\boldsymbol{\lambda}\cdot(\boldsymbol{V}+\boldsymbol{\xi}\times\boldsymbol{r})\mathrm{d}\boldsymbol{x} \tag{2}$$

$$\int_{P(t)}[\boldsymbol{u}-(\boldsymbol{U}+\boldsymbol{\omega}\times\boldsymbol{r})]\cdot\varsigma\mathrm{d}\boldsymbol{x}=0 \tag{3}$$

Continuity equation:

$$\int_{V_0}q\nabla\cdot\boldsymbol{u}\mathrm{d}\boldsymbol{x}=0 \tag{4}$$

In the above equations, $\boldsymbol{u}$, p, $\boldsymbol{\lambda}$, $\boldsymbol{U}$, $\boldsymbol{\omega}$ are the fluid velocity, fluid pressure, distributed Lagrange multiplier, particle translational velocity, and particle rotational velocity, respectively, and $\boldsymbol{v}$, q, $\boldsymbol{\xi}$, $\boldsymbol{V}$, and ς are their corresponding variations. $\boldsymbol{D}$ denotes the fluid rate-of-strain tensor. ρ_{r} is the particle-fluid density ratio. Re denotes the Reynolds number defined by $Re=\rho_{\mathrm{f}}U_{\mathrm{c}}L_{\mathrm{c}}/\eta$, here ρ_{f}, U_{c}, L_{c} and η being the fluid density, the characteristic velocity, the characteristic length and the fluid viscosity, respectively. Fr represents the Froude number defined by $Fr=gL_{\mathrm{c}}/U_{\mathrm{c}}^{2}$, g being the gravitational acceleration. V_{p}^{*} and J^{*} are the dimensionless particle area (in case of two-dimension) and moment of inertia, defined by $V_{\mathrm{p}}^{*}=M/\left(\rho_{\mathrm{s}}L_{\mathrm{c}}^{2}\right)$ and $J^{*}=J/\left(\rho_{\mathrm{s}}L_{\mathrm{c}}^{4}\right)$, here ρ_{s}, M and J are the dimensional particle density, mass and moment of inertia, respectively. $\boldsymbol{r}$ is the position vector with respect to the particle mass center.

The fractional time step scheme is used to decouple the original system (1)—(4) to two sub-system: the fluid Navier-Stokes problem and the Lagrange multiplier problem. The fluid Navier-Stokes equation problem is solved with the projection method on a half-staggered grid, and the Lagrange multiplier problem is solved with the Uzawa iterative method. The reader is referred to Yu *et al*.[22] for the detailed description of the algorithm.

The computation is performed on a rectangular domain covering the outer cylinder wall. The no-slip boundary conditions on both cylinder walls are enforced

with another set of Lagrange multiplier.

2.3 Computational parameters

The particle diameter d and Ωd are taken as the characteristic length and velocity respectively. Thus, the dimensionless rotational velocity of the inner cylinder is unity. From the dimensional analysis, the dimensionless parameter group comprises (k, R^*, ρ_r, Re, Fr). Here R^* is the dimensionless outer cylinder radius, *i.e.*, the ratio of the outer cylinder radius to the particle diameter. Throughout this study, $k=0.25$, $R^*=20$, $\rho_r=1.0001$ and $Fr=0$ are fixed. The above values of ρ_r and Fr are chosen because it is not intended to inspect the effect of gravity. The singularity of Eq.(2) at $\rho_r=1.0$ does not permit the calculation of the velocity of the particles with the density exactly matching the fluid density. However, it has been shown that the particles are essentially neutrally-buoyant as long as ρ_r is close to unity and Fr is close to zero[20].

Four simulations with different parameter values are performed in an attempt to examine the effects of the volume fraction and inertia, as listed in Table 1. For convenience, the four cases are referred to as LRLV (Lower Reynolds number and Lower Volume fraction), HRLV (Higher Reynolds number and Lower Volume fraction), LRHV, and HRHV, respectively.

Table 1 Simulation cases considered in this study

Cases	Fluid	Re	ϕ	Number of particles
LRLV	Newtonian	0.01	0.371	556
HRLV	Newtonian	0.1	0.371	556
LRHV	Newtonian	0.01	0.464	696
HRHV	Newtonian	0.1	0.464	696

The mean volume fractions for 556 particles and 696 particles are 0.371 and 0.464, respectively. However, it is rather difficult to generate a random particle concentration distribution over the entire domain initially at relatively high volume fractions. Therefore, a regular particle distribution at initial time is given, as shown in Fig.3. The concentration distribution is taken as a function of radial position and is obtained by computing the area occupied by particles in annular regions (see Fig.2). Due to the defect of the initial particle distribution near both cylinders (Fig.3), the volume concentrations will not be considered at these two positions and the initial concentrations at other positions are about 0.4 and 0.5 respectively.

The spatial resolution used is 512×512 and the time step is $\pi/1000$.

3 SIMULATION RESULTS

The chain-like particle clustering has been observed in simple shear flow[8]. The reason for such clustering is that there are interactions (approach, collision and departure) between particles due to inhomogeneous velocity distribution in shear flow, and during the interactions the particles spend more time staying in the compression axis direction than in other

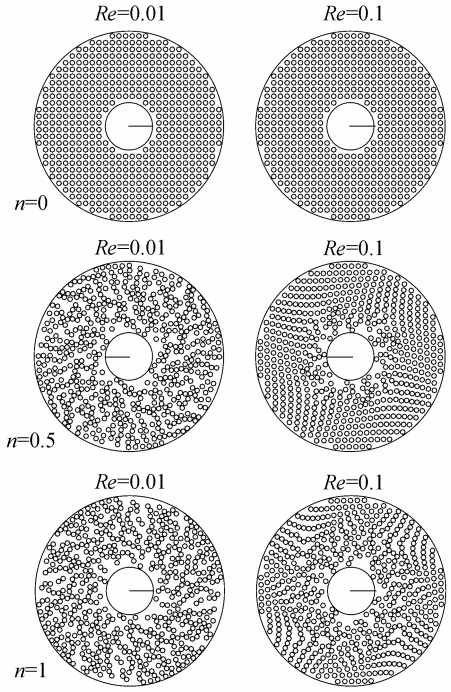

Figure 3 Snapshots of particles for LRLV and HRLV at early stage (within the first turn, n is the number of turns in all figures)

direction, resulting in a predominance of clusters aligned with the compression axis at any observation time (see Figs.3—5). The presence of such an orientational predominance of chain clusters was recognized as a mechanism for the observation that the measured transient viscosity of the suspension in the circular Couette device was decreased upon the reversal of the rotational direction of the inner wall[8]. Note that such clustering is not a stable particle gathering process, as caused by the attractive forces between the particles, but is rather a manifestation of inhomogeneous particle distribution due to shear flow. The clusters are not compact but loose ones, and their exact sizes are difficult to determine. The clustering is a dynamic process, since it can be conceived that the chain clusters continually break down and re-form due to the velocity difference between particles.

The snapshots of particles for different cases in our simulations of particle motion in circular Couette flow are presented in Figs.3—5. The circular Couette flow is an inhomogeneous shear flow with the highest shear-rate at the inner cylinder wall and the lowest shear-rate at the outer cylinder wall. The particle collision (or clustering) takes place with the higher frequency at the region of higher shear rate, *i.e.*, closer to the inner cylinder. From Figs.3—5, chain (or column)-like clustering of particles is present in all cases, and the clusters are more aligned with the flow direction as the radial position increases (or the shear rate decreases), and there is a tendency for particles near the outer cylinder to pack into concentric rings (Fig.5), unlike the case of simple shear flow. The particle arrangement into concentric rings has also been observed in a bimodal suspension in a circular Couette

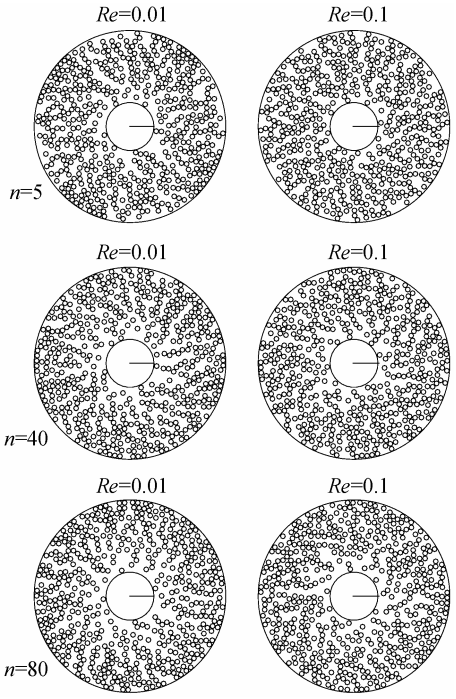

Figure 4 Snapshots of particles for LRLV and HRLV after a few turns

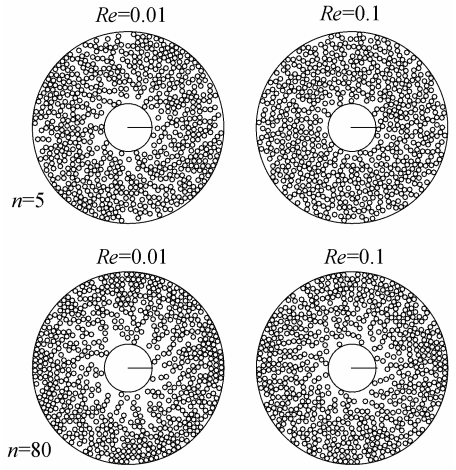

Figure 5 Snapshots of particles for LRHV and HRHV

device experimentally by Graham *et al*.[9], as shown in Fig.1. Clearly, the hydrodynamic drag on particles is minimum for such an arrangement.

The evolutions of volume fractions as a function of radial position are plotted in Fig.6. It is indicated that the particles migrate from the higher shear rate region near the inner cylinder towards the lower shear rate region near the outer cylinder in call cases. At early times ($n=5$), the particle migration taking place at the region in the vicinity of the inner cylinder is much more pronounced than near the outer cylinder, which is consistent with the experimental observations (Abbott *et al*.[2]). It is believed that the formation of chain-like clusters near the inner cylinder is responsible for the rapid decrease in particle concentration there at this early stage, which will be further discussed late for the case of Poiseuille flow.

Figure 6 (as well as Figs.3—5) shows that inertia has a negative effect on particle migration. The inertial effect is most pronounced at early times. Fig.3 reveals that it takes more dimensionless time to completely fluidize the particles at a higher Reynolds number, probably due to the higher particle inertia at higher *Re*.

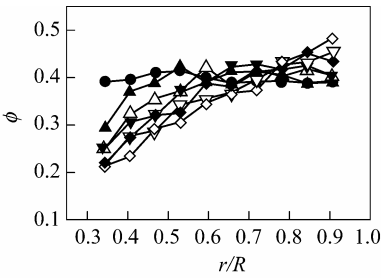

(a) LRLV and HRLV

● $n=0$; △ LRLV, $n=5$; ▽ LRLV, $n=40$; ◇ LRLV, $n=80$; ▲ HRLV, $n=5$; ▼ HRLV, $n=40$; ◆ HRLV, $n=80$

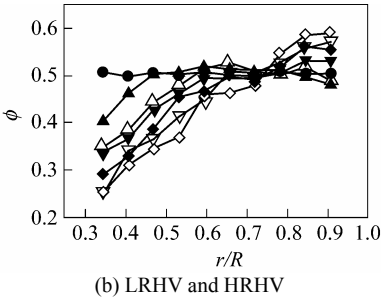

(b) LRHV and HRHV

● $n=0$; △ LRHV, $n=5$; ▽ LRHV, $n=40$; ◇ LRHV, $n=80$; ▲ HRHV, $n=5$; ▼ HRHV, $n=40$; ◆ HRHV, $n=80$

Figure 6 Comparisons of the evolutions of volume fractions between LRLV and HRLV, LRHV and HRHV

Figure 7(a) shows the streamlines and particle distribution for the case of LRLV and $n=5$, and Fig.7(b) presents the close-up of Fig.7(a) at the region marked with a small box, plus the velocity vector plot. It can be seen that the presence of particles does not produce a significantly inhomogeneous flow field, which is not surprising since the flow is shear flow, the particles are neutrally buoyant, the particle concentration is not high enough to cause jam, and in particular the Reynolds number is low. In the close-up plot [Fig.7(b)], one may find that there is always a gap between closely-spaced particles, the reason being that a repulsive force is activated to prevent the penetration

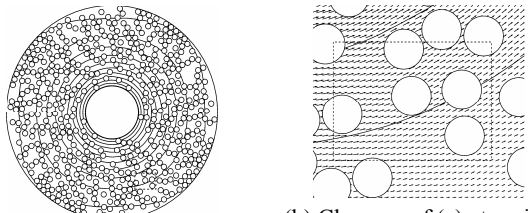

(a) Streamlines and particle distribution

(b) Close-up of (a) at region marked with a small box, plus the velocity vector plot

Figure 7 A case of LRLV and $n=5$

of two approaching particles when the gap is smaller than a critical distance.

In order to further inspect the role of clustering in the particle migration at early stage, the case of Poiseuille flow of a Newtonian fluid is investigated. The particle diameter and the velocity at the centerline are taken as the characteristic length and the characteristic velocity respectively. The size of the computational domain is 20×20. 192 particles are initially arranged into 14 rows, and the even rows and the odd rows are staggered by two grids in the streamwise direction, as shown in Fig.8. This pattern is not symmetric about the centerline, thus one should not expect the symmetry of the particle pattern about the centerline during the evolution. The Reynolds number is set to be 0.1 and the flow flux is kept constant during the simulation. The spatial resolution used is 256×256 and the time step is 0.01.

Figure 8 shows that clustering occurs at the higher shear rate region first and gradually involves particles at the lower shear rate region. In the formation of clusters, the particles locating at the inward end of the clusters are pushed inwards, which, on one hand, reduces the local particle volume fraction, and on the other hand, disturbs the previously regularly spaced arrays of particles, resulting in the inward spread of the clustering instability.

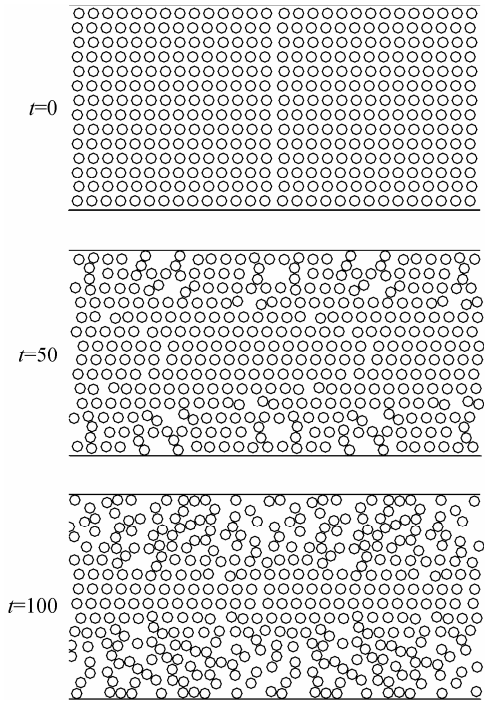

Figure 8 Snapshots of circular particles in a plane Poiseuille flow (The domain is duplicated in the streamwise direction with a periodic boundary condition)

4 CONCLUSIONS

The shear-induced migration of circular particles in a two-dimensional circular Couette flow has been simulated numerically with a distributed Lagrange multiplier based fictitious domain method. The effects of inertia and volume fraction on the particle migration have been examined. The results indicate that inertia has a negative effect on the particle migration, and it takes more dimensionless time to completely fluidize the particles at a higher Reynolds number. In consistence with the experimental observations, the rapid migration of particles near the inner cylinder at the early stage is observed in this simulation, which is believed to be related to the chain-like clustering of particles. The migration of circular particles in a plane Poiseuille flow is also examined in order to further confirm the effect of such clustering on the particle migration at early stage. There is tendency for the particles in the vicinity of outer cylinder in the Couette device to pack into concentric rings at late stage in case of high particle concentration.

NOMENCLATURE

$\boldsymbol{D}$	dimensionless fluid rate-of-strain tensor
d	particle diameter, m
Fr	Froude number
g	gravitational acceleration, $\mathrm{m\cdot s^{-2}}$
J	particle moment of inertia, $\mathrm{kg\cdot m^2}$
J^*	dimensionless particle moment of inertia
k	ratio of outer cylinder to inner cylinder
L_c	characteristic length, m
M	particle mass, kg
P	interior of the particles
p	dimensionless fluid pressure
q	variation for the fluid pressure
R	radius of the outer cylinder, m
R^*	dimensionless radius of the outer cylinder
Re	Reynolds number, $Re=\rho_f U_c L_c/\eta=\rho_f \Omega d^2/\eta$
$\boldsymbol{r}$	dimensionless position vector with respect to particle mass center
t	dimensionless time
$\boldsymbol{U}$	dimensionless particle translational velocity
U_c	characteristic velocity, $\mathrm{m\cdot s^{-1}}$
$\boldsymbol{u}$	dimensionless fluid velocity
$\boldsymbol{V}$	variation for the particle translational velocity
V_P^*	dimensionless particle volume
V_0	entire computational domain
$\boldsymbol{v}$	variation for the fluid velocity
ς	variation for the particle rotational velocity
η	fluid viscosity, $\mathrm{kg\cdot m^{-1}\cdot s^{-1}}$
$\boldsymbol{\lambda}$	dimensionless distributed Lagrange multiplier
$\boldsymbol{\xi}$	variation for the distributed Lagrange multiplier
ρ_f	fluid density, $\mathrm{kg\cdot m^{-3}}$
ρ_r	particle-fluid density ratio
ρ_s	particle density, $\mathrm{kg\cdot m^{-3}}$
ϕ	particle volume fraction
Ω	angular velocity of the inner cylinder, $\mathrm{s^{-1}}$
$\boldsymbol{\omega}$	dimensionless particle rotational velocity

REFERENCES

1 Leighton, D., Acrivos, A., "The shear-induced migration of particles in concentrated suspensions", *J. Fluid Mech*., **181**, 415—439(1987).

2 Abbott, J.R., Tetlow, N., Graham, A.L., Altobelli, S.A., Fukushima, E., Mondy, L.A., Stephens, T.S., "Experimental observations of particle migration in concentrated suspensions: Couette flow", *J. Rheol*., **35**, 773—795(1991).

3 Lyon, M.K., Leal, L.G., "An experimental study of the motion of concentrated suspensions in two-dimensional channel flow (Ⅰ) Monodisperse systems", *J. Fluid Mech*., **363**, 25—56(1998).

4 Phillips, R.J., Armstrong, R.C., Brown, R.A., Graham,A.L., Abbott, J.R., "A constitutive equation for

concentrated suspensions that accounts for shear-induced particle migration", *Phys. Fluids A*, **4**, 30—40(1992).
5 Tetlow, N., Graham, A.L., Ingber, M.S., Subia, S.R., Mondy, L.A., Altobelli, S.A., "Particle migration in a Couette apparatus: Experiment and modeling", *J. Rheol.*, **42**, 307—327(1998).
6 Nott, P.R., Brady, J.F., "Pressure-driven flow of suspensions: Simulation and theory", *J. Fluid Mech.*, **275**, 157—199(1994).
7 Fang, Z., Mammoli, A.A., Brady, J.F., Ingber, M.S., Mondy, L.A., Graham, A.L., "Flow-aligned tensor models for suspension flows", *Int. J. Multiphase Flow*, **28**, 137—166(2002).
8 Leighton, D., Rampall, I., "Measurement of the shear-induced microstructure of concentrated suspensions of noncolloidal spheres", In: Particulate Two-Phase Flow, Butterworth-Heinemann, 190—209(1993).
9 Graham, A.L., Altobelli, S.A., Fukushima, E., Mondy, L.A., Stephens, T.S., "Note: NMR imaging of shear-induced diffusion and structure in concentrated suspensions undergoing Couette flow", *J. Rheol.*, **35**, 191—201(1991).
10 Gao, J., Xu, C., Yang, G., Guo, Y., Lin, W. "Numerical simulation on gas-solid two-phase turbulent flow in FCC riser reactors (Ⅰ) Turbulent gas-solid flow-reaction model", *Chin. J. Chem. Eng.*, **6**(1), 12—20(1998).
11 Shang, Z., Yang, R., Fukuda, K.J., Zhong, Y., Ju, Z., "A numerical simulation of gas-particle two-phase flow in a suspension bed using diffusion flux model", *Chin. J. Chem. Eng.*, **11**(5), 497—503(2003).
12 Luo, K., Zheng, Y., Fan, J., Cen, K., "Interaction between large-scale vortex structure and dispersed particles in a three dimensional mixing layer", *Chin. J. Chem. Eng.*, **11**(4), 377—382(2003).
13 Wang, W., Li, T., "Simulation of the clustering phenomenon in a fast fluidized bed: The importance of drag correlation", *Chin. J. Chem. Eng.*, **12**(3), 335—341(2004).
14 Liu, C., Guo, Y., "Mechanisms for particle clustering in upward gas-solid flows", *Chin. J. Chem. Eng.*, **14**(2), 141—148(2006).
15 Hu, H.H., Patankar, A., Zhu, M.Y., "Direct numerical simulations of fluid solid systems using the arbitrary Lagrangian-Eulerian technique", *J. Comput. Phys.*, **169**, 427—462(2001).
16 Ladd, A.J.C., Verberg, R., "Lattice-Boltzmann simulations of particle-fluid suspensions", *J. Stat. Phys.*, **104**, 1191—1251(2001).
17 Glowinski, R., Pan, T.W., Hesla, T.I., Joseph, D.D., "A distributed Lagrange multiplier/fictitious domain method for particulate flows", *Int. J. Multiphase Flow*, **25**, 755—794(1999).
18 Glowinski, R., Pan, T.W., Hesla, T.I., Joseph, D.D., Periaux, J., "A fictitious domain approach to the direct numerical simulation of incompressible viscous flow past moving rigid bodies: Application to particulate flow", *J. Comput. Phys.*, **169**, 363—426(2001).
19 Yu, Z., Phan-Thien, N., Fan, Y., Tanner, R.I., "Viscoelastic mobility problem of a system of particles", *J. Non-Newt. Fluid Mech.*, **104**, 87—124(2002).
20 Yu, Z., Phan-Thien, N., Tanner, R.I., "Dynamic simulation of sphere motion in a vertical tube", *J. Fluid Mech.*, **518**, 61—93(2004).
21 Yu, Z., "A DLM/FD method for fluid/flexible-body interactions", *J. Comput. Phys.*, **207**, 1—27(2005).
22 Yu, Z., Wachs, A., Peysson, Y., "Numerical simulation of particle sedimentation in shear-thinning fluids with a fictitious domain method", *J. Non-Newt. Fluid Mech.*, **136**, 126—139(2006).
23 Yu, Z., Shao, X., Wachs, A., "A fictitious domain method for particulate flows with heat transfer", *J. Comput. Phys.*, **217**, 424—452(2006).